



# Nickel nanoparticles supported on graphene as catalysts for aldehyde hydrosilylation

Juan F. Blandez<sup>a</sup>, Iván Esteve-Adell<sup>a</sup>, Ana Primo<sup>a</sup>, Mercedes Alvaro<sup>a</sup>, Hermenegildo García<sup>a,b,\*</sup>

<sup>a</sup> Instituto Universitario de Tecnología Química CSIC-UPV and Departamento de Química, Univ. Politécnica de Valencia, Av. de los Naranjos s/n, 46022 Valencia, Spain

<sup>b</sup> Center of Excellence for Advanced Materials Research, King Abdullah University of Science and Technology, Jeddah, Saudi Arabia



## ARTICLE INFO

### Article history:

Received 18 September 2015  
Received in revised form  
11 November 2015  
Accepted 12 November 2015

### Keywords:

Heterogeneous catalysis  
Nickel nanoparticles  
Graphene as support  
Aldehyde hydrosilylation

## ABSTRACT

Nickel nanoparticles (NPs) supported on different undoped or doped with N or B graphenes (Gs) have been tested as catalyst for the hydrosilylation of aldehydes to obtain the corresponding siloxanes with high conversion and good selectivity in short reaction time. The different Gs employed were obtained by pyrolysis under inert atmosphere of alginate or chitosan, modified or not with boric acid. Then the metal NPs obtained by polyol reduction method using ethylene glycol were adsorbed on Gs. The Ni-containing G catalysts were characterized by electron microscopy, XPS and Raman spectroscopy. The scope of the Ni/G catalyst includes aliphatic and aromatic aldehydes as well as a variety of hydrosilanes.

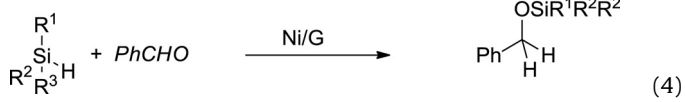
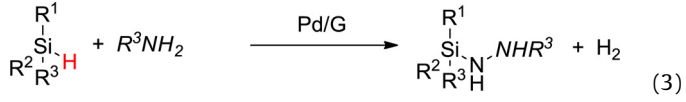
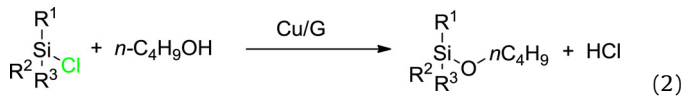
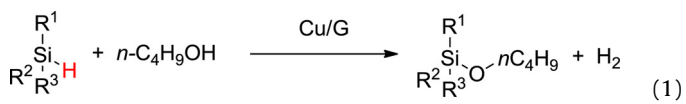
© 2015 Elsevier B.V. All rights reserved.

## 1. Introduction

Due to its large surface area, extended  $\pi$  orbitals, 2D morphology and high dispersability, graphene (G) and related materials are suitable supports of metal nanoparticles (MNPs) exhibiting high catalytic activity [1–7]. In some cases, it has been found that the activity of MNPs supported on G is better than the activity of these MNPs on other supports including different types of carbon nanoforms and metal oxides [3,4,7,8]. On one hand, overlap between the  $p$  and  $d$  orbitals of transition metal with  $\pi$  orbitals of G can modulate the electronic density on the MNPs and also may result in a strong metal–support interaction necessary to avoid leaching and minimize MNP size growth. On the other hand, the adsorption capacity of G bringing substrates and reagents near the active MNP can contribute to increase the reaction rates.

Recently, we have reported that Cu NPs supported on G is a highly efficient catalyst to promote the dehydrogenative coupling of alcohol with hydrosilanes (Eq. (1)) [9]. This reaction has the advantage over the conventional silylation (Eq. (2)) of overcoming the use of halosilanes and minimizing the production of corrosive byproducts (HX), increasing atom efficiency. Although Pd exhibits

higher activity than Cu for the oxidative coupling of silanes and alcohols, Cu as catalyst has advantages in terms of affordability and sustainability. Similarly, the dehydrogenative coupling of hydrosilanes and amines (Eq. (3)) has also been recently reported using Pd supported on G as catalyst [10]. For both processes, it was found that G as support leads to a more efficient catalyst than when the MNPs are deposited on other materials.



Continuing with this line of research aimed at exploiting the potential of Gs as support of MNPs, in the present manuscript we describe that Ni NPs supported on G is a convenient catalyst for

\* Corresponding author at: Center of Excellence for Advanced Materials Research, King Abdullah University of Science and Technology, Jeddah, Saudi Arabia. Fax: +966 34963877809.

E-mail address: [hgarci@qim.upv.es](mailto:hgarci@qim.upv.es) (H. García).

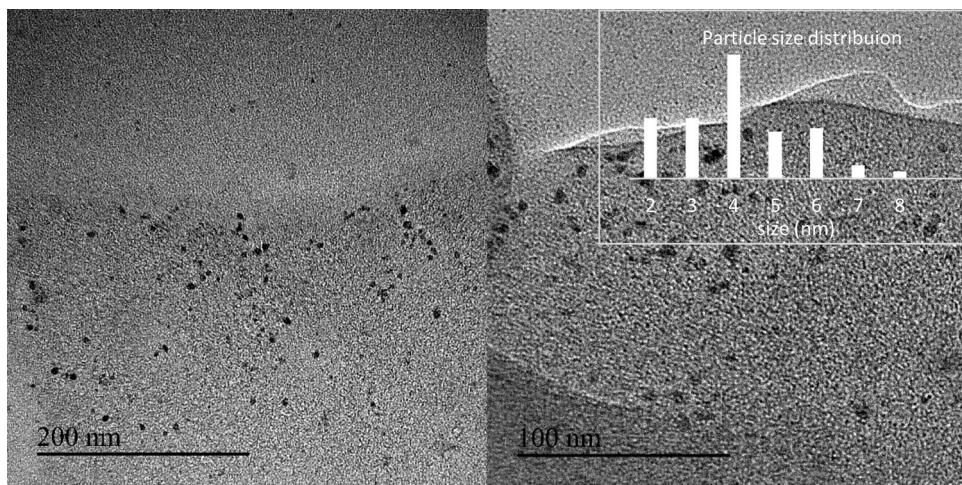


**Fig. 1.** Two TEM images at different magnification taken for Ni/G. The inset shows the size distribution of Ni NPs.

the addition of silanes to aromatic aldehydes. This reaction (Eq. (4)) is similar to the Strecker addition of halosilanes to aldehydes catalyzed by diluted acids. Also in this case, the hydrosilylation has the advantage of avoiding halosilanes as reagents.

## 2. Experimental

### 2.1. Catalysts synthesis and characterization

As supports of MNPs and based on related precedents for the dehydrogenative coupling of hydrosilanes and alcohols or amines [9,10], a G obtained by exfoliation of turbostratic graphitic carbon obtained by pyrolysis of alginate was used. In addition, B- and N-doped Gs [(B)G and (N)G, respectively] were obtained pyrolyzing the borate ester of alginate [(B)G] or chitosan [(N)G] at 1000 °C under inert atmosphere, followed by exfoliation of the graphitic carbon residues by sonication [11–13]. For the sake of comparison graphene oxide (GO) prepared from graphite by Hummers oxidation and exfoliation was also included as support in the study [14].

All these Gs are well documented in the literature and had been previously used as metal-free catalysts or as support of MNPs [9,10,15–17]. The G samples employed in the present study were characterized by TEM, AFM, Raman and XPS and their properties coincide with those reported in the literature for these G samples [10,18–21].

MNPs were obtained by the polyol method consisting in the reduction of salts of the corresponding metals in hot ethylene glycol [22]. Deposition was performed simultaneously to the formation of the MNPs by suspending the corresponding G in ethylene glycol at the same time that the reduction of the metal ions is taking place [22]. In the present study, MNPs of Cu, Ni and Pd supported on various Gs were prepared. The Cu/G and Pd/G catalysts correspond to those samples previously reported in the literature [9,10]. G-supported catalysts were analyzed to determine the metal content that was 5 wt% in all cases. TEM allowed determining the morphology and average MNP size and XPS was used to establish the oxidation state of Ni. The single layer morphology of Ni/G was established by AFM.

The Ni NPs employed as catalysts for the addition reaction between the aldehyde and the hydrosilane were supported on the G samples following the synthesis described in the literature [10]. Accordingly, a suspension in ethylene glycol of graphene and the metal precursor, NiCl<sub>2</sub>, was sonicated for 1 h. After sonication the mixture was heated at 120 °C for 24 h at reflux temperature. Ni NPs

are formed by reduction of ethylene glycol and becoming spontaneously deposited on G in the same step.

### 2.2. Catalytic tests

The corresponding catalyst (0.06 mmol% of metal respect to substrate) was introduced in an ampoule equipped with a magnetic bar. The aldehyde (10 mmol) was added under argon atmosphere and the ampoule was sonicated for 30 min. Then, hydrosilane (5 mmol) and dodecane as internal standard were added to the ampoule and the reactor sealed. The reaction mixture was magnetically stirred at 120 °C in an oil bath preheated at the reaction temperature. At the end of the reaction, the reaction mixture was cooled to room temperature and an aliquot of 0.1 mL was diluted with anhydrous toluene (0.5 mL), filtered, and injected into GC, determining the conversion and product yields based on the internal standard. The rest of the reaction mixture was filtered and the liquid phase diluted in deuterated chloroform and analysed by <sup>1</sup>H NMR spectroscopy (Varian Gemini 300 MHz) to determine product selectivity. Supporting information contains spectroscopic data of the hydrosilylation products **3a–h**.

## 3. Results and discussion

As support of MNPs and based on related precedents for the dehydrogenative coupling of hydrosilanes and alcohols or amines [9,10], a G obtained by exfoliation of turbostratic graphitic carbon resulting from pyrolysis of alginate was initially used. Two additional doped Gs, (B)G and (N)G, were obtained pyrolyzing at 1000 °C under inert atmosphere the borate ester of alginate [(B)G] and chitosan [(N)G], followed by exfoliation of the graphitic carbon residues by sonication [11,13]. For the sake of comparison GO prepared from graphite by Hummers oxidation and exfoliation was also included as support in the study [14].

All these Gs are well documented in the literature and had been previously used either as metal-free catalysts or as support of MNPs [9,10,15–17]. The G samples employed in the present study were characterized by chemical analysis, TEM, AFM, Raman and XPS and their properties coincide with those reported in the literature for these G sample [10,18–21].

MNPs were obtained by the polyol method consisting in the reduction of the salts of the corresponding metals in hot ethylene glycol [22]. Deposition was performed simultaneously to the formation of the MNPs by suspending G in ethylene glycol at the same time that the reduction of the metal ions was taking place [22]. In

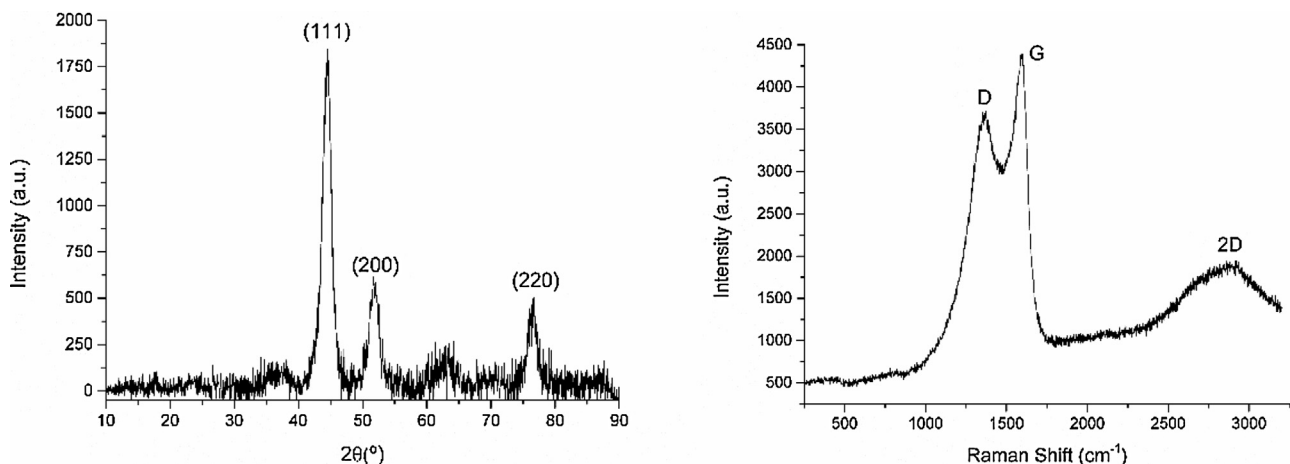


**Fig. 2.** XRD and Raman spectrum for the Ni/G sample used as catalyst.

the present study, MNPs of Cu, Ni and Pd supported on various Gs were prepared. The Cu/G and Pd/G catalysts correspond to those samples previously reported in the literature [9,10]. G-supported catalysts were characterized by: (i) chemical analysis to determine the metal content, that was 3.2 wt%, (ii) TEM allowed to determine the morphology and average MNP size, and (iii) XPS was used to establish the oxidation state of Ni. The single layer morphology of Ni/G was established by AFM.

Fig. 1 shows two representative TEM images recorded for Ni/G and the histogram of the Ni NP size distribution that gives an average dimension of 4 nm. The average particle size estimated by statistical analysis of TEM images coincide with the average particle size calculated from XRD pattern of Ni/G (Fig. 2) using the width of the most intense (1 1 1) peak corresponding to Ni metal by applying the Scherrer equation.

XPS measurements showed the presence of Ni and C in the Ni/G sample. Fig. 3 presents the experimental high resolution C 1s and Ni 2p recorded for Ni/G and the best deconvolution to individual components. According to this analysis there are three types of C at binding energy (BE) values of 287.7, 284.5 and 282.5 eV in a atomic proportion of 7, 41 and 37%, respectively. While the two components with the higher BE can be safely attributed to C atoms bonded to O and graphenic C, respectively, the component with the lowest BE value is unusual. We attribute this component to graphenic C interacting with Ni NPs and having higher electron density than expected for G. This assignment is in agreement with the observation in XPS that the BE values for Ni atoms is higher than for metallic Ni. Thus, the high resolution Ni peak in XPS could be resolved into two peaks at BE values of 855.7 and 854.0 eV with a relative atomic proportion of 0.2 and 0.1%, respectively. These BE values are unusually high for Ni(0) that should appear at about 852 eV. Thus, the data of XPS suggesting Ni(II) does not seem to fit with those of XRD indicating Ni(0). One possibility to reconcile these two conflicting experimental data for the Ni oxidation state is to assume that XPS is probing the external layers of Ni NPs that have become oxidized by ambient O<sub>2</sub>. However this external NiO passivating Ni NPs should be very thin compared to the size of metallic Ni(0), since NiO is undetectable in XRD. Therefore, XRD will report on the majority of Ni atoms and XPS on the thin shell. Alternatively, it could be that the charge transfer that causes a 2 eV shift to lower BE in one component of graphenic C (37%) would be also responsible for the apparent 2 eV higher value of Ni(0). This proposal will imply an interaction between Ni NPs and G, strong enough to shift the BE value of certain C and Ni atoms in close contact. Whatever the reason, it appears that the Ni supported on G has electron deficiency and has positive character.

Besides on G, Ni NPs were also supported on (N)G and (B)G. In the literature there are theoretical calculations as well as experimental data showing that the presence of heteroatoms on G can increase the interaction of this support with MNPs, providing a strong anchoring of Ni NPs on G and modulating the electronic density of the MNPs [23]. In addition, heteroatoms on G, such as B or N, can act as active centers in the reaction mechanism cooperating to the catalysis [24–29]. For the sake of comparison, the present study also includes Cu NPs supported on (N)G and (B)G that correspond to the samples already reported [9].

### 3.1. Catalytic activity

In the initial stage of our work, the addition of dimethylphenylsilane (**1a**) to benzaldehyde (**2a**) to form benzyloxyphenyldimethylsilane (**3a**) was selected and proceeded to optimization of the reaction conditions and screening of the catalyst activity of the various samples. The results obtained are summarized in Table 1.

Cu/G has been found previously a good catalyst for the dehydrogenative silylation of alcohols [9] and, therefore, it was an obvious candidate to check as catalyst for aldehyde hydrosilylation. As it can be seen in Table 1, while under certain conditions Cu/G can promote a high conversion of silyl ethers (high Cu ratio, 120 °C), the selectivity toward the target compound was always unsatisfactory due to the formation of disiloxane (**4a**). Under other conditions, selectivity to the addition product **3a** using Cu/G could be high (see Table 1, entry 2), but, then, conversion was unsatisfactorily low. The use of N(G) or B(G) as supports instead of G does not appear to play a crucial role enhancing the performance of Cu. In contrast to Cu catalysts, Pd/G was able to achieve complete conversion with essentially complete selectivity in very short reaction times (Table 1, entry 18). Besides Pd, we were interested in determining whether or not affordable, first-row transition metals could also lead to high yields and selectivity toward **3a**. Aimed at this purpose the activity of Ni/G was screened at temperatures between 80 and 140 °C and loadings from 0.012 to 0.06 mol% (Table 1, entries 9–17). As it can be seen in Table 1, using Ni/G at 120 °C and working at 0.06 mol% of Ni, very high conversions with almost complete selectivity were attained already at 3 h reaction time, conversion and selectivity increasing slightly from 3 to 5 h reaction time (Table 1, entries 10 and 11). Fig. 4 shows the temporal evolution of **1a** conversion and **3a** yield using Ni/G as catalyst (0.06 mol%) under optimal conditions. Decreasing the temperature results not only in lower conversion for 24 h reaction time, but also in a lower selectivity to **3a** due to the formation of disiloxane (**4a**). Decreasing Ni to substrate mol ratio from 0.06 to 0.012 leads to a remarkable high

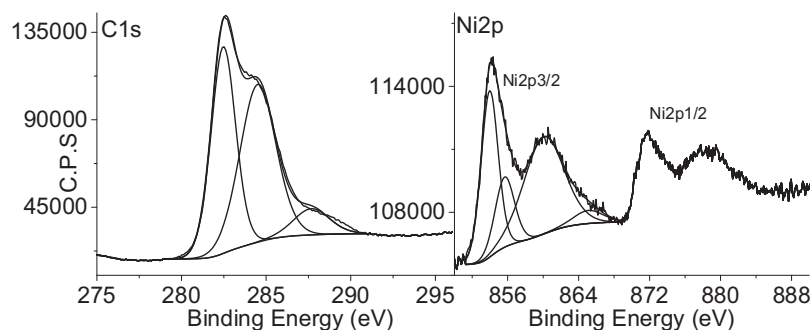


**Fig. 3.** High resolution C 1s and Ni 2p XPS peaks of Ni/G and their best deconvolution to three (C) and two (Ni) components.

**Table 1**

Results of the catalytic addition of dimethylphenylsilane (**1a**) to benzaldehyde (**2a**) in the presence of different catalysts with or without MNPs supported on G.

Entry	Catalyst	T (°C)	t (h)	Load (mol%)	Conversion of <b>1a</b> <sup>b</sup> (%)	Selectivity to <b>3a</b> <sup>b</sup> (%)
1	Cu/G	120	24	0.06	64	80
2	Cu/G	120	48	0.06	68	95
3	Cu/G	50	24	0.06	48	73
4	Cu/G	50	168	0.06	54	72
5	Cu/G	120	3	0.06	26	79
6	Cu/G	120	3	0.12	94	39
7	Cu/(N)G	120	24	0.06	39	56
8	Cu/(B)G	120	24	0.06	73	94
9	Ni/G	120	24	0.06	100	99
10	Ni/G	120	3	0.06	96	99
11	Ni/G	120	5	0.06	100	99
12	Ni/G	100	24	0.06	88	78
13	Ni/G	80	24	0.06	77	78
14	Ni/G	120	24	0.012	84	96
15	Ni/G	120	48	0.012	97	96
16	Ni/(N)G	120	24	0.06	60	68
17	Ni/(B)G	120	24	0.06	86	96
18	Pd/G	120	0.08	0.06	100	99
19	GO	120	24	–	0	0
20	(N)G	120	24	–	20	47
21	(B)G	120	24	–	30	78

<sup>a</sup> Reaction conditions: **1a** (5 mmol), **2a** (10 mmol), catalyst (0.06 mol%), *n*-dodecane as internal standard (0.1 mmol), Ar atmosphere.

<sup>b</sup> Conversion and selectivity were determined by GC based on calibration with internal standard.

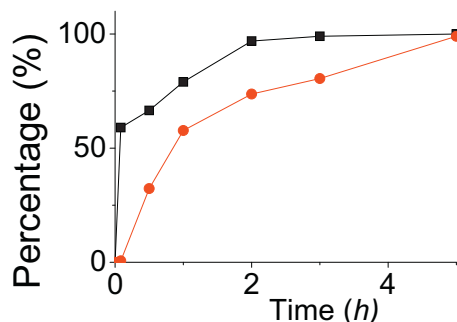


**Fig. 4.** Time-conversion of **1a** (■) and time-yield (●) of **3a** plots for the hydrosilylation of **2a** by **1a**. Reaction conditions: **1a** (5 mmol), **2a** (10 mmol), catalyst (0.1 mol%), dodecane as internal standard (0.1 mmol), Ar atmosphere, 120 °C.

conversion and selectivity, although much longer reaction times are required to reach almost complete conversion. The maximum turnover number achieved for the addition of phenyldimethylsilane (**1a**) to benzaldehyde (**2a**) using Ni/G as catalyst in the present study was  $10^5$  measured at 20 days reaction time working at 120 °C reaction temperature with a Ni to substrate mol ratio of

0.0006 mol%. As observed for the case of the Cu/G the presence of N or B heteroatoms on G was detrimental for the catalytic performance, being this negative influence particularly notable in the case of (N)G. It could be that in the present case the presence of N or B heteroatoms on G influences the electronic density of Ni NPs by heteroatom–Ni interactions and this result in a less active sites.

The activation energy (Ea) for the addition of hydrosilane **1a** to benzaldehyde (**2a**) using Cu/G or Ni/G was determined using the Arrhenius plot from the influence of the temperature on the initial reaction rate. As an example, Fig. 5 shows the Arrhenius plot for the reaction between **1a** and **2a** catalyzed by Ni/G catalyst, while the time-conversion plots at different temperatures from which the initial reaction rates were determined are presented as an inset of this figure. The Ea values obtained for Ni/G and Cu/G were 19.8 and 31.5 kJ/mol, respectively, indicating the higher catalytic activity of Ni/G compared to Cu/G.

A reusability test was performed by recovering the Ni/G catalyst after the reaction, washing it with hexane and drying it at room temperature. The used Ni/G catalyst was resuspended by sonication in a fresh reaction medium. This test shows that the Ni/G catalyst undergoes strong deactivation during the reaction. While almost a complete conversion was achieved for the fresh

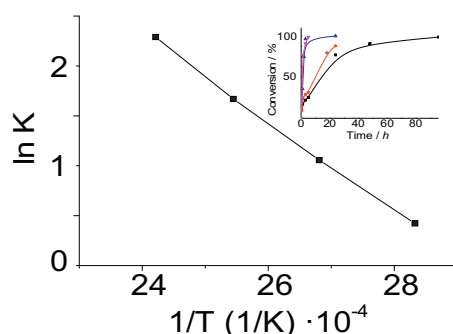


**Fig. 5.** Arrhenius plot for the reaction between **1a** and **2a** catalyzed by Ni/G. The inset shows the time-conversion plots at 80, 10, 120 and 140 °C from which the initial reaction rates ( $k$ ) were calculated.

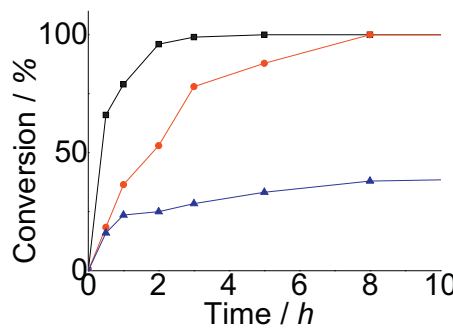


**Fig. 6.** Time-conversion plot for three consecutive uses of the same Ni/G catalyst. First use ■, second use ●, and third use ▲.

catalyst in 3 h, to achieve complete conversion in the second and third runs 8 and 168 h were necessary, respectively. Fig. 6 shows the time-conversion plots for three consecutive uses of the same Ni/G sample.

ICP analysis of the liquid phase after removal of the Ni/G catalyst indicated that Ni leaching is not the cause of deactivation since the percentage of the initial Ni that migrated to the solution was only about 1% of the Ni content of the Ni/G catalyst. TEM images of the three-times used catalyst show the presence of Ni NPs, supported on the carbon layers without much apparent increase in the average particle size as determined by statistical analysis of the average particle size of images of sufficient magnification. The most likely reason for the strong deactivation of Ni/G catalyst upon use seems to be the change in the 2D morphology of the G sheets as consequence of folding and wrapping of the sheet to form a 3D object. Fig. 7 presents selected TEM images to illustrate these changes in the morphology of the Ni/G upon its use as catalysts. As it can be seen in these images, the 2D morphology of G is not clearly observed after its use as catalyst and most probably G undergoes corrugation leading to 3D objects by folding and wrapping of the 2D sheet.

The scope of Ni/G as catalyst was screened by performing the carbonyl addition using various hydrosilanes and aldehydes. The results obtained are summarized in Table 2. This table shows that besides hydrosilane **1a**, other silanes also give high conversion and selectivity to the corresponding siloxanes (Table 2, entries 2 and 3) and only when the bulky triphenylsilane (**1d**) was used as reagent the addition product was not formed (Table 2, entry 4), probably due to the strong steric encumbrance. The only product observed in the reaction using triphenylsilane (**1d**) as reagent was the corresponding triphenylsilanol. On the other hand, when different aldehydes were used as substrates with the dimethylphenylsilane (**1a**) longer reaction times were necessary to achieve high conversions. In agreement with a reaction mechanism involving a nucleophilic attack to the carbonyl group, when aldehydes have an electron donor group as substituent on the ring, the conversion decreased and longer reaction times were necessary to achieve high conversions (Table 2, entry 7). Nevertheless, the selectivity to the expected *O*-benzylsiloxane **3** was not excessively influenced by the electron density of the ring and moderate selectivity values toward the addition product were obtained for substituted benzaldehydes having both electron donor or acceptor substituents (Table 2,

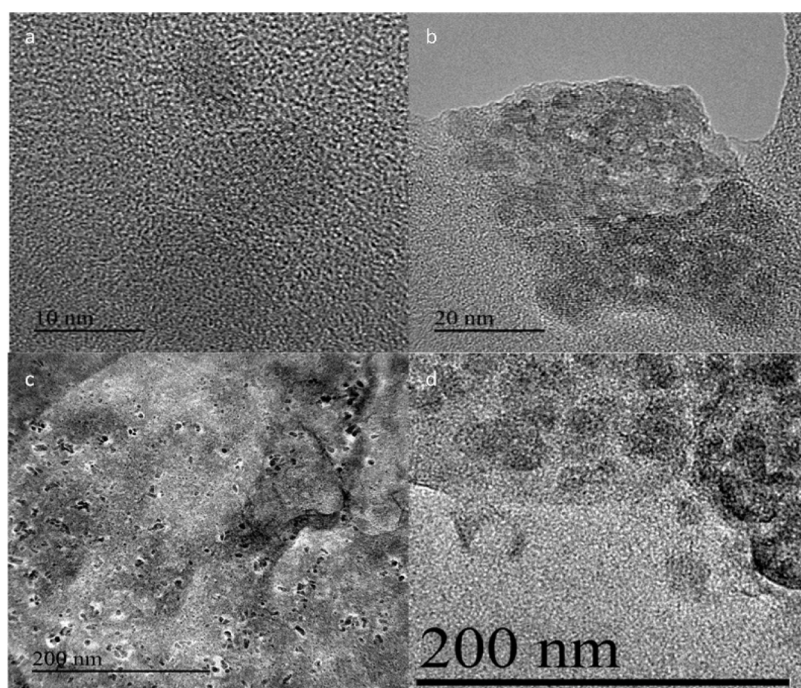


**Fig. 7.** TEM images at different magnifications taken for the Ni/G sample after being used three times as catalyst panels (a) and (b) show that the average Ni nanoparticles size has not changed with respect to the fresh catalyst. Frame (c) presents a broader view of the sample. Panel (d) shows folding of the graphene sheet.

**Table 2**Catalytic activity of Ni/G for hydrosilylation of silanes and aldehydes.<sup>a</sup>

Entry	Silane	Aldehyde	Time	Product	Conver <sup>b</sup> (%)	Selec <sup>c</sup> (%)
1	(1a)	(2a)	5	(3a)	100	99
2	(1b)	(2a)	5	(3b)	100	81
3	(1c)	(2a)	5	(3c)	100	80
4 <sup>d</sup>	(1d)	(2a)	5	(3d)	100	0
5	(1a)	(2b)	24	(3e)	100	70
6	(1a)	(2c)	24	(3f)	98	70
7	(1a)	(2d)	48	(3g)	95	76
8	(1a)	(2e)	24	(3h)	98	65
9 <sup>e</sup>	(1a)	(2f)	24	(3i)	15	0

<sup>a</sup> Reaction conditions: silane (5 mmol), aldehyde (10 mmol), catalyst (0.06 mol%), dodecane as internal standard (0.1 mmol), Ar atmosphere, temperature 120 °C.<sup>b</sup> Conversion was determined by GC using internal standard.<sup>c</sup> Selectivity was determined by <sup>1</sup>H NMR spectroscopy.<sup>d</sup> Only triphenylsilanol was formed.<sup>e</sup> **2f** (6 mmol).

entries 7 and 8). Aliphatic aldehydes were also tested (**Table 2**, entries 5 and 6), attaining high conversions with good selectivity. Among the aldehydes tested, only furfuraldehyde failed to afford the expected hydrosilylation product (**Table 2**, entry 9).

#### 4. Conclusions

The present study has shown that Ni NPs (4 nm average particle size) supported on G are conveniently prepared by reducing  $\text{Ni}^{2+}$  salt in ethylene glycol containing G [22]. Ni/G is general catalyst to promote the hydrosilylation of aldehydes with high selectivity, reaching TON of  $10^5$  and exhibiting relatively low activation energy, while Cu/G failed to catalyze this reaction. Ni/G promotes the addition in a wide range of substituted hydrosilanes and aromatic and aliphatic aldehydes. Although Ni/G becomes deactivated during the course of the reaction, no Ni leaching or Ni particle size is observed. The main deactivation pathway appears to be the loss of the 2D morphology of G as observed in TEM images. The catalytic activity of Ni/G compares to that of Pd/G and constitutes an example of how noble metals can be substituted as catalysts for abundant and affordable base transition metals.

#### Acknowledgments

Financial support by the Spanish Ministry of Economy and Competitiveness (Severo Ochoa and CTQ2012-32315) and Generalitat Valenciana (Prometeo 2013-019) is gratefully acknowledged. J.F.B. and I.E.A. thanks to the Technical University of Valencia and the Spanish Ministry of Economy and Competitiveness for postgraduate scholarships, respectively.

#### References

- [1] L. Greb, S. Tamke, J. Paradies, *Chem. Commun.* 50 (2014) 2318–2320.
- [2] C.D.F. Konigs, M.F. Muller, N. Aiguabella, H.F.T. Klare, M. Oestreich, *Chem. Commun.* 49 (2013) 1506–1508.
- [3] J.A. Zazo, J.A. Casas, A.F. Mohedano, J.J. Rodríguez, *Appl. Catal. B: Environ.* 65 (2006) 261–268.
- [4] S. Ikeda, S. Ishino, T. Harada, N. Okamoto, T. Sakata, H. Mori, S. Kuwabata, T. Torimoto, M. Matsumura, *Angew. Chem. Int. Ed.* 118 (2006) 7221–7224.
- [5] P.V. Kamat, *J. Phys. Chem. Lett.* 1 (2010) 520–527.
- [6] C. Xu, X. Wang, J. Zhu, *J. Phys. Chem. C* 112 (2008) 19841–19845.
- [7] L. Shang, T. Bian, B. Zhang, D. Zhang, L.Z. Wu, C.H. Tung, Y. Yin, T. Zhang, *Angew. Chem. Int. Ed.* 53 (2014) 250–254.
- [8] J. Sirijaraensreab, J. Limtrakul, *Phys. Chem. Chem. Phys.* 17 (2015) 9706–9715.
- [9] J.F. Blandez, A. Primo, A.M. Asiri, M. Álvaro, H. García, *Angew. Chem. Int. Ed.* 53 (2014) 12581–12586.
- [10] J.F. Blandez, I. Esteve-Adell, A. Primo, M. Álvaro, H. García, *Catal. Sci. Technol.* 5 (2015) 2167–2173.
- [11] A. Dhakshinamoorthy, A. Primo, P. Concepcion, M. Alvaro, H. Garcia, *Chem. Eur. J.* 19 (2013) 7547–7554.
- [12] M. Latorre-Sánchez, A. Primo, H. García, *Angew. Chem. Int. Ed.* 52 (2013) 11813–11816.
- [13] I. Lazareva, Y. Koval, M. Alam, S. Strömsdörfer, P. Müller, *Appl. Phys. Lett.* 90 (2007) 262108-1–262108-3.
- [14] S. Hummers Wm, E. Richard Offeman Jr., *J. Am. Chem. Soc.* 80 (1958) 1339.
- [15] H. Wang, L. Thia, N. Li, X. Ge, Z. Liu, X. Wang, *Appl. Catal. B* 166–167 (2015) 25–31.
- [16] S. Guo, S. Zhang, L. Wu, S. Sun, *PCT Int. Appl.* (2014) 26.
- [17] S. Guo, S. Sun, *J. Am. Chem. Soc.* 134 (2012) 2492–2495.
- [18] T. Kuila, S. Bose, A.K. Mishra, P. Khanra, N.H. Kim, J.H. Lee, *Prog. Mater. Sci.* 57 (2012) 1061–1105.
- [19] C. Soldano, A. Mahmood, E. Dujardin, *Carbon* 48 (2010) 2127–2150.
- [20] H. Wang, T. Maiyalagan, X. Wang, *ACS Catal.* 2 (2012) 781–794.
- [21] Y. Zhu, S. Murali, W. Cai, X. Li, J.W. Suk, J.R. Potts, R.S. Ruoff, *Adv. Mater.* 22 (2010) 3906–3924.
- [22] W.-J. Ong, L.-L. Tan, S.-P. Chai, S.-T. Yong, *Dalton Trans.* 44 (2015) 1249–1257.
- [23] E. Yoo, T. Okata, T. Akita, M. Kohyama, J. Nakamura, I. Honma, *Nano Lett.* 9 (2009) 2255–2259.
- [24] X. Chen, L. Wan, J. Huang, L. Ouyang, M. Zhu, Z. Guo, X. Yu, *Carbon* 68 (2014) 462–472.
- [25] R. Li, Z. Wei, X. Gou, W. Xu, *RSC Adv.* 3 (2013) 9978–9984.
- [26] H. Wang, Y. Zhou, D. Wu, L. Liao, S. Zhao, H. Peng, Z. Liu, *Small* 9 (2013) 1316–1320.
- [27] X. Wang, X. Li, L. Zhang, Y. Yoon, P.K. Weber, H. Wang, J. Guo, H. Dai, *Science* 324 (2009) 768–771.
- [28] Z. Yang, Z. Yao, G. Li, G. Fang, H. Nie, Z. Liu, X. Zhou, X. Chen, S. Huang, *ACS Nano* 6 (2011) 205–211.